

Controlling domain wall nucleation and injection through focussed ion beam irradiation in perpendicularly magnetized nanowires

A. Beguivin, D. C. M. C. Petit, R. Mansell, and R. P. Cowburn

Citation: *AIP Advances* **7**, 015203 (2017); doi: 10.1063/1.4974465

View online: <http://dx.doi.org/10.1063/1.4974465>

View Table of Contents: <http://aip.scitation.org/toc/adv/7/1>

Published by the [American Institute of Physics](#)

Articles you may be interested in

[The mechanical response in a fluid of synthetic antiferromagnetic and ferrimagnetic microdiscs with perpendicular magnetic anisotropy](#)

AIP Advances **110**, 042402042402 (2017); 10.1063/1.4974211

[The effect of underlayers on the reversal of perpendicularly magnetized multilayer thin films for magnetic micro- and nanoparticles](#)

AIP Advances **121**, 043908043908 (2017); 10.1063/1.4974300

[Magnetic domain-wall creep driven by field and current in Ta/CoFeB/MgO](#)

AIP Advances **7**, 055918055918 (2017); 10.1063/1.4974889

[On the magnetic anisotropy in Fe₇₈Si₉B₁₃ ingots and amorphous ribbons: Orientation aligning of Fe-based phases/clusters](#)

AIP Advances **7**, 015302015302 (2017); 10.1063/1.4974305

HAVE YOU HEARD?

Employers hiring scientists and
engineers trust

PHYSICS TODAY | JOBS

www.physicstoday.org/jobs



Controlling domain wall nucleation and injection through focussed ion beam irradiation in perpendicularly magnetized nanowires

A. Beguivin, D. C. M. C. Petit, R. Mansell,^a and R. P. Cowburn
*Cavendish Laboratory, University of Cambridge, JJ Thomson Avenue,
 Cambridge CB3 0HE, United Kingdom*

(Received 24 October 2016; accepted 5 January 2017; published online 18 January 2017)

Using Ga⁺ focussed ion beam irradiation of Ta/Pt/CoFeB/Pt perpendicularly magnetized nanowires, the nucleation and injection fields of domain walls into the nanowires is controlled. The nucleation and injection fields can be varied as a function of dose, however, the range of injection fields is found to be limited by the creation of a step in anisotropy between the irradiated and unirradiated regions. This can be altered by defocussing the beam, which allows the injection fields to be further reduced. The ability to define an arbitrary dose profile allows domain walls to be injected at different fields either side of an asymmetrically irradiated area, which could form the initial stage of a logic device. The effect of the thickness of the magnetic layer and the thickness of a Ta underlayer on the dose required to remove the perpendicular anisotropy is also studied and is seen that for similar Ta underlayers the dose is determined by the thickness of the magnetic layer rather than its anisotropy. This finding is supported by some transport of ions in matter simulations. © 2017 Author(s). All article content, except where otherwise noted, is licensed under a Creative Commons Attribution (CC BY) license (<http://creativecommons.org/licenses/by/4.0/>). [<http://dx.doi.org/10.1063/1.4974465>]

INTRODUCTION

Magnetic nanowires have been widely studied due to possible applications in data storage and logic.^{1,2} A domain wall separating two magnetic domains in a nanowire has shown great promise as a memory or logic bit due to the ability to move them at high speeds and to manipulate the properties of the domain walls.^{3–5} Recently, focus has turned to perpendicularly magnetized materials where the large out-of-plane anisotropies lead to very narrow domain walls, which are particularly promising for technological applications.^{6,7} It has been shown that these walls can have very high velocities when driven by both fields and in-plane currents.^{8,9}

One requirement of these designs is the controlled injection of domain walls into the nanowires. Various methods to achieve this have been demonstrated including local Oersted fields,⁶ manipulation of the in-plane shape^{10,11} and irradiation by focussed ion beam (FIB).^{12,13} FIB irradiation of perpendicular materials has been shown to reduce the anisotropy of the irradiated area, largely by causing intermixing of the heavy metal/magnetic interfaces which provide the perpendicular anisotropy.¹⁴ The perpendicular anisotropy is a competition between an interfacial magnetocrystalline anisotropy and the demagnetizing energy of the layer. This effective anisotropy can be written as $K_{\text{eff}} = K_0 - (\mu_0 M_s^2)/2$, where K_0 is given by the strength of the interfacial anisotropy (from the combined effect of the two interfaces), μ_0 is the vacuum permeability and M_s the saturation magnetization. The perpendicular anisotropy reduces much more rapidly than the saturation magnetization of the material with increasing ion dose. It is expected that a local reduction in anisotropy caused by FIB irradiation will provide a preferential nucleation site for reversed domains.^{13,15} The domain walls created by reversing the irradiated area with reduced anisotropy can then be used as bits for data storage or logic applications.

^aElectronic mail: rm353@cam.ac.uk

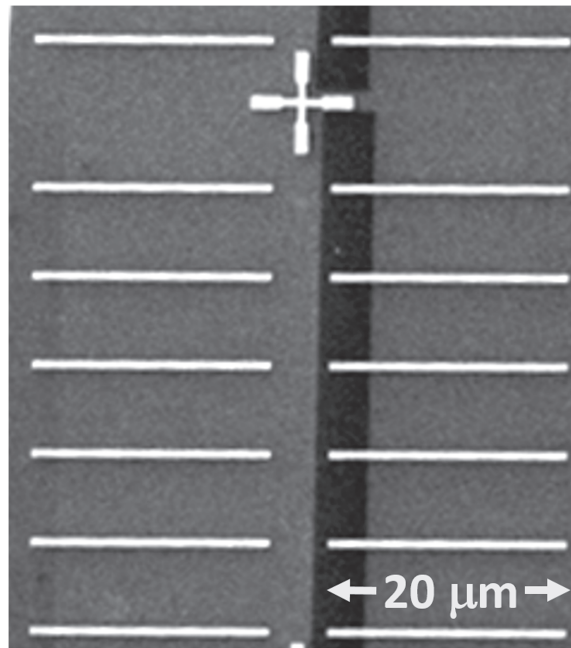


FIG. 1. SEM image of a series of 500 nm wide, 20 μm long nanowires with irradiated areas on the left hand side seen through a change in colour.

In this paper we study the domain wall injection properties of FIB irradiated perpendicularly magnetized nanowires, distinguishing between the nucleation fields of reversed domains in the irradiated part and the field required to inject the domain wall into the unirradiated nanowire. We show that by varying the dose the domain wall injection field changes systematically and that by designing asymmetric irradiation profiles, domain walls can be injected into two sides of the same wire at different fields. The effects of changing the thicknesses of the magnetic layers and the Ta underlayer are also studied.

METHODS

The wires studied have a width of 500 nm and a general layer structure of Ta/Pt/CoFeB/Pt. The wires are patterned using a lift-off technique with PMMA and e-beam lithography. An SEM image of part of an array of irradiated wires is shown in figure 1. The darker patches on the left-hand side of the wires show the irradiated area. Irradiation is carried out with an FEI Helios NanoLab dual beam system. Data shown in this paper is taken from averages of 12 wires unless stated otherwise.

DOMAIN WALL NUCLEATION AND INJECTION

In figure 2(a) a typical set of switching field versus dose plots for nucleation and injection fields is given for perpendicularly magnetized Ta (4 nm)/Pt (10 nm)/CoFeB (0.6 nm)/Pt (2 nm) nanowires measured by focussed polar magneto-optical Kerr effect (MOKE) magnetometry. The switching field of an unirradiated nanowire is shown by the horizontal blue line. As the ion dose is initially increased both the nucleation and injection fields decrease. This means that when a reversed domain is nucleated in the irradiated part it immediately propagates along the wire. This trend continues until, at around 1.5×10^{13} ions/cm³, the two fields diverge.¹⁶ In the polar MOKE measurement this is seen as a two step hysteresis loop corresponding to the two fields (not shown). As the dose increases further the nucleation field decreases until the effective perpendicular anisotropy in the irradiated wire is extinguished and this region of the wire has in-plane magnetization. This

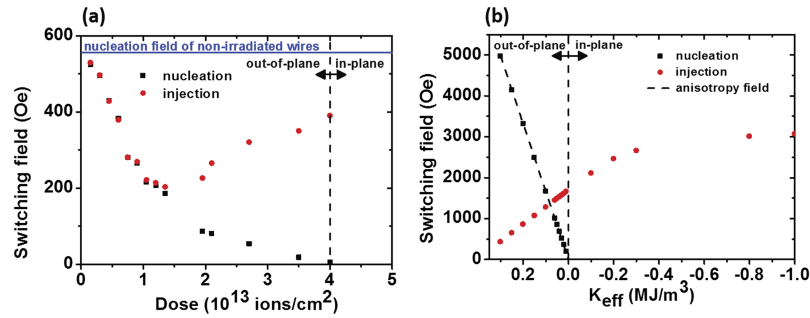


FIG. 2. (a) The injection and nucleation fields of Ta (4 nm)/Pt (10 nm)/CoFeB (0.6 nm)/Pt (2 nm) nanowires as a function of dose. Only one end of the nanowire is irradiated. (b) Simulated nucleation and injection fields at 0 K using a 200 nm long area of reduced perpendicular anisotropy.

is the expected effect of the FIB irradiation due to reduction of perpendicular anisotropy from the intermixing of the CoFeB/Pt interfaces by the Ga⁺ bombardment. The lower anisotropy leads to lower nucleation fields until the perpendicular anisotropy is overcome by the demagnetizing energy and the magnetization lies in-plane. The injection field, however, after it diverges from the nucleation field, increases for increasing dose. To understand this behavior micromagnetic simulations were carried out, shown in figure 2(b). A 500 nm wide wire was used with a 200 nm long section given a reduced anisotropy, K_0' . For the rest of the wire an interfacial perpendicular anisotropy, K_0 , of 1.3 MJ/m³ was used, with an M_s of 1.2×10^6 A/m, which leads to an effective perpendicular anisotropy of 0.4 MJ/m³. Figure 2(b) is plotted in terms of the effective anisotropy of the reduced anisotropy region going from perpendicular to in-plane magnetized. Two different sets of simulations with varying K_0' were carried out. Firstly, the magnetic field required to reverse the region of lowered anisotropy was found. To do this the wire was initially negatively saturated then a positive applied field was increased in steps of 10 Oe, with an in-plane field along the wire of 5 Oe in order to break the symmetry, until the irradiated part reversed (black squares). The nucleation field closely follows the effective anisotropy field of the wire, also marked in figure 2(b). Secondly, the simulation was started with the section with lowered anisotropy already reversed and the field required to propagate the reversed domain wall along the remaining wire was found (red circles). It should be noted that these are 0 K simulations so, as would be expected, the nucleation and propagation fields are much higher than in room temperature experiments.¹⁷ However, there is a clear qualitative agreement between the simulation and experiment. Firstly, reducing the anisotropy leads to a reduction in the nucleation field until the magnetization lies in plane. Secondly, the injection field is a monotonically increasing function of the reduction of anisotropy even into the region where there is in-plane anisotropy. In the experiment we cannot probe the injection field until it is at higher field than the nucleation field, giving rise to the nucleation and injection fields tracking each other at low doses. The reason for the increasing injection field is the creation of a step in anisotropy of increasing size between the irradiated and unirradiated areas.¹⁶ As the difference in the anisotropy increases so does the field required to overcome the difference. This shows that it is possible to tune the injection field of a domain wall into a nanowire with FIB, but only within a certain range due to this effect. The issue is apparent (see figure 2(a)) if we note that in this layer structure we are unable to inject a domain wall at less than 200 Oe, even though the nucleation field can be made arbitrarily small.

One way to change the injection properties and to circumvent the issue described above is to change the boundary between the irradiated and unirradiated regions.^{12,16} In the experimental data described above the region between the two parts of the nanowire was defined by the Gaussian width of the FIB beam. This is around 3.5 nm at the focal point of the beam. This width can be effectively increased by defocusing the beam by moving the sample stage relative to the focal point. The effect of defocusing on the injection field is shown in figure 3. This experiment was carried out on a Ta (4 nm) / Pt (6 nm) / CoFeB (0.6 nm) / Pt (2 nm) sample. The range of ion doses used leads to the dosed region having in-plane magnetization. There is no reduction in the domain wall injection

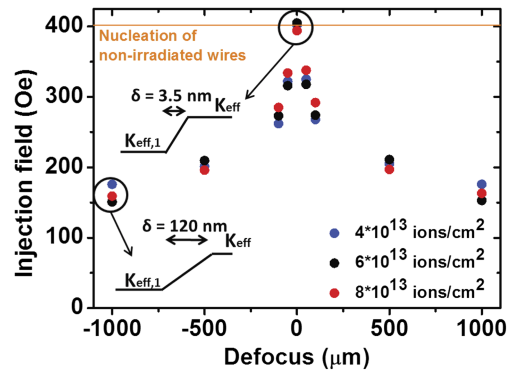


FIG. 3. Injection fields for a Ta (4 nm) / Pt (6 nm) / CoFeB (0.6 nm) / Pt (2 nm) sample with doses of 4×10^{13} ions/cm³ (blue), 6×10^{13} ions/cm³ (black), and 8×10^{13} ions/cm³ (red) as a function of the defocus of the sample stage.

field at no defocus, probably due to nucleation elsewhere in the wire. By increasing the defocus the domain wall injection field reduces. The defocussing increases the width of the transition region and so reduces the rate of change of the anisotropy, allowing injection from the in-plane region.¹³

ASYMMETRIC DEVICES

One way to take advantage of this effect is to create designed irradiation profiles. This could allow, for example, one nucleation patch to lead to domain walls nucleating at different fields to the left and right, forming part of a simple domain wall logic device.¹⁸ Such a device is shown in figure 4. In figure 4(a) average switching fields of the device to the left and right of the irradiated area are shown. In the center of the figure is the schematic of the device with the ten different radiation

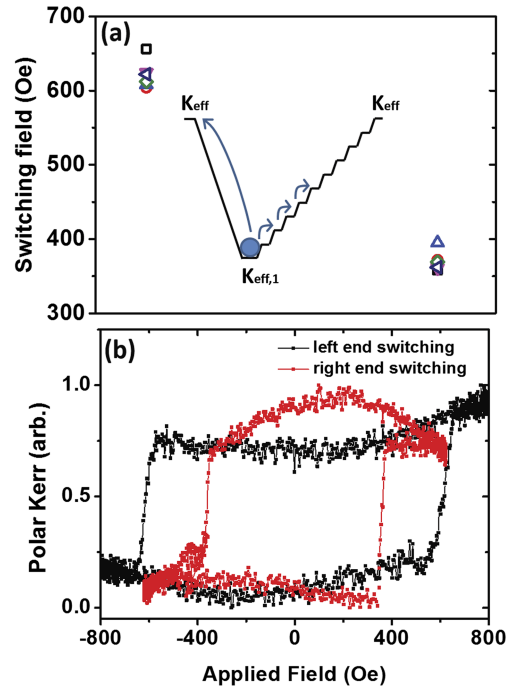


FIG. 4. (a) Injection fields to the left and right of the asymmetrically irradiated area for 6 different nanowire devices (different symbols). Inset: Schematic of the ion dose profile. (b) Illustrative hysteresis loops showing the asymmetry in switching between the left and right hand ends of the irradiated nanowire.

doses used to create a particular lateral anisotropy profile, which is shown schematically in the inset of figure 4(a). Each irradiated section is $100\ \mu\text{m}$ across. The profile is strongly asymmetric with a much sharper transition on the left-hand side between the most irradiated section and the unirradiated area than on the right-hand side which has a graded profile. The profile is created with a fully focussed FIB beam, which gives a greater control of the profile than the defocussed beam in figure 3. In figure 4(b) hysteresis loops are shown for one wire, where it is seen that the right-hand side of the wire switches at more than 600 Oe, whilst the left-hand side switches at less than 400 Oe, allowing selective propagation of the domain walls created by the reversal of the irradiated area.

EFFECT OF CoFeB AND Ta LAYER THICKNESSES

A further interesting matter for the use of FIB irradiation for controlling nanowire properties is the effect of the layer structure. There are several points to take into account. For a given set of underlayers and capping layers thicker magnetic layers have lower anisotropy because the out-of-plane anisotropy is an interfacial effect. However, changing the underlayers can also effect the anisotropy. In figure 5 atomic force microscopy images are shown of an 8 nm thick Pt layer grown directly on Si (figure 5(a)) or with a 2 nm Ta buffer (figure 5(b)). As can be seen the inclusion of a Ta buffer causes a considerable reduction in the roughness of the Pt layer. This will also enhance the perpendicular anisotropy of a magnetic layer grown on top.^{19,20} However, increasing the Ta thickness further can lead to reductions in perpendicular anisotropy as the Ta layer changes from amorphous to polycrystalline with increasing thickness.

The effect of changing the Ta layer, along with changing the CoFeB thickness is studied in figure 6. Firstly, in figure 6(a) the change in nucleation field as a function of dose is shown for four different multilayer structures with data averaged over six wires per point. Three of the wires are of the form Ta (4 nm) / Pt (6 nm) / CoFeB (x) / Pt (2 nm) with x of 0.6 nm, 0.7 nm and 0.8 nm and the fourth wire has Ta (2 nm) / Pt (6 nm) / CoFeB (0.6 nm) / Pt (2 nm). For the samples with 4 nm Ta layers, the anisotropies are $0.87\ \text{MJ/m}^3$, $0.70\ \text{MJ/m}^3$, and $0.57\ \text{MJ/m}^3$ for the 0.6 nm, 0.7 nm and 0.8 nm layers, respectively, and $0.98\ \text{MJ/m}^3$ for the sample with a 2 nm Ta underlayer. The anisotropies were derived from the hard axis saturation field measured on thin films and it is assumed that patterning into 500 nm nanowires does not strongly affect these values.

As can be seen from figure 6(a) the samples with higher anisotropy require a lower ion dose to become in-plane magnetized, with the two highest anisotropies not distinguishable. This is quite surprising, and indeed it has been suggested previously that the trend should be opposite to this.¹³ The conclusion from this data is that, for the range of thickness studied here, the thickness of the ferromagnetic layers determines the dose required to put the magnetization in-plane not the initial value of the anisotropy.

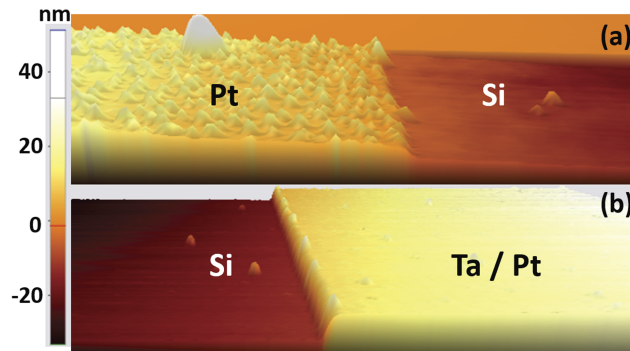


FIG. 5. Three-dimensional rendition of an atomic force microscopy image of an 8 nm Pt layer (a) grown directly on Si and (b) grown on a 2 nm Ta buffer on Si.

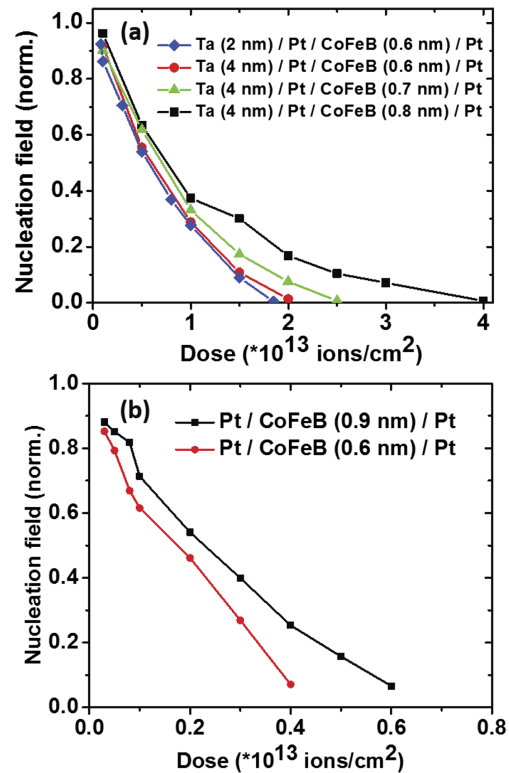


FIG. 6. (a) Trends in nucleation field with increasing ion dose for a series of nanowires of different layer structure, normalized to the injection field without irradiation. (b) Nucleation field as a function of dose for two layers without Ta underlayers, normalized to the injection field without irradiation.

In figure 6(b) two sets of wires without Ta buffers are measured. Compared to figure 6(a) the required doses to cause the magnetism to lie in plane are significantly lower. This is because the effective perpendicular anisotropy of these layers is significantly lower than the same magnetic layer thickness with a Ta buffer. For the 0.6 nm CoFeB layer the effective perpendicular anisotropy is 0.25 MJ/m^3 , and for the 0.9 nm CoFeB layer 0.07 MJ/m^3 . However, the same effect of changing the magnetic layer thickness is seen here. The 0.9 nm CoFeB requires a higher dose to cause the magnetization to lie in plane.

Support for the idea that for a given set of underlayers the thicker magnetic layer may require higher doses before the magnetization lies in plane is supported by some exploratory transport of ions in matter (TRIM) simulations.²¹ Using a Ta (4 nm) / Pt (10 nm) / CoFeB (0.6/0.9 nm) / Pt (2 nm) stack with an incoming beam of Ga⁺ ions at 25 keV the number of vacancies and replacement collisions is simulated. The CoFeB is modelled as an amorphous layer with the same Co₆₀Fe₂₀B₂₀ composition as the films used in this study. At the top Pt / CoFeB interface the two data sets are very similar. For the lower CoFeB/Pt interface, which has been shown to provide the majority of the perpendicular anisotropy²² there is a marked divergence in vacancies of the Co and Fe atoms. For the thicker CoFeB layer there are 2.2 vacancies per ion for Co atoms and 0.7 vacancies per ion for Fe atoms compared to 2.5 (Co) and 0.9 (Fe) vacancies per ion for the thinner layer.

This suggests that the slight difference in CoFeB thickness leads to considerably less intermixing of the Pt/CoFeB bottom interface. This may in part be due to this interface being slightly further from the top interface. However, there is likely to be a complex interaction due to the fact that each ion causes multiple collisions. For instance, the number of replacement collisions, where an atom knocked off its position is replaced by an atom from the same layer, at the bottom interface is 0.7 replacement collisions/ion for the 0.9 nm CoFeB and only 0.3 collisions/ion for the 0.6 nm layer. Another notable feature of the simulations is that the stopping range of the ions in Pt is very short, peaking around 5 nm for the energy used here. This means that the effective dose can be controlled over

quite a large range by altering the capping layer thickness. The sensitivity to the thickness parameters shown here provides another way to optimize the interaction of ion beams with perpendicular layers in order to control the nucleation and injection of domain walls.

CONCLUSION

In conclusion, the properties of the nucleation and propagation of domain walls in perpendicularly magnetized nanowires has been studied as a function of Ga⁺ ion dose. It has been found that the injection field of domain walls can be controlled by dose to some extent. The step in anisotropy between irradiated and unirradiated regions leads to higher domain wall injection fields and reduces the range of injection fields that can be obtained through this technique. This can be partly overcome by changing the rate of change of anisotropy with distance. It has been shown by defocussing the beam that lower injection fields can be obtained and then by using a designed dose pattern at full focus the ability to inject domains at different field either side of a nucleation site of a nanowire was shown. Lastly, the effect of changing the magnetic layer thickness and Ta underlayer thickness was studied. For similar Ta underlayers it was seen that the dose required to put the magnetization in plane depends on the thickness of the layer rather than the initial anisotropy, a result supported by TRIM simulations. The experiments combine to show the versatility of FIB irradiation in controlling the properties of perpendicular thin films, which remains a promising avenue for the rapid prototyping of future magnetic devices.

ACKNOWLEDGMENTS

This research was funded by the European Community under the Seventh Framework Program ERC Contract No. 247368: 3SPIN, and by EMRP JRP EXL04 SpinCal. The EMRP is jointly funded by the EMRP participating countries within EURAMET and the EU. AB acknowledges DTA funding from the EPSRC.

- ¹ D. A. Allwood, G. Xiong, C. C. Faulkner, D. Atkinson, D. Petit, and R. P. Cowburn, *Science* **309**, 1688 (2005).
- ² S. S. P. Parkin, M. Hayashi, and L. Thomas, *Science* **320**, 190 (2008).
- ³ D. A. Allwood, G. Xiong, M. D. Cooke, C. C. Faulkner, D. Atkinson, N. Vernier, and R. P. Cowburn, *Science* **296**, 2003 (2002).
- ⁴ R. P. Cowburn, D. A. Allwood, G. Xiong, and M. D. Cooke, *Journal of Applied Physics* **91**, 6949 (2002).
- ⁵ Y. Zhang, W. S. Zhao, D. Ravelosona, J.-O. Klein, J. V. Kim, and C. Chappert, *Journal of Applied Physics* **111**, 093925 (2012).
- ⁶ K.-J. Kim, J.-C. Lee, S.-J. Yun, G.-H. Gim, K.-S. Lee, S.-B. Choe, and K.-H. Shin, *Applied Physics Express* **3**, 083001 (2010).
- ⁷ J. Jaworowicz, N. Vernier, J. Ferré, A. Maziewski, D. Stanescu, D. Ravelosona, A. S. Jacqueline, C. Chappert, B. Rodmacq, and B. Diény, *Nanotechnology* **20**, 215401 (2009).
- ⁸ T. A. Moore, I. M. Miron, G. Gaudin, G. Serret, S. Auffret, B. Rodmacq, A. Schuhl, S. Pizzini, J. Vogel, and M. Bonfim, *Applied Physics Letters* **93**, 262504 (2008).
- ⁹ K.-S. Ryu, L. Thomas, S.-H. Yang, and S. Parkin, *Nature Nanotechnology* **8**, 526 (2013).
- ¹⁰ J. Kimling, T. Gerhardt, A. Kobs, A. Vogel, S. Wintz, M.-Y. Im, P. Fischer, H. P. Oepen, U. Merkt, and G. Meier, *Journal of Applied Physics* **113**, 163902 (2013).
- ¹¹ R. Mansell, A. Beguivin, D. C. M. C. Petit, A. Fernández-Pacheco, J. H. Lee, and R. P. Cowburn, *Applied Physics Letters* **107**, 092405 (2015).
- ¹² J. H. Franken, M. Hoeijmakers, R. Lavrijsen, J. T. Kohlhepp, H. J. M. Swagten, B. Koopmans, E. van Veldhoven, and D. J. Maas, *Journal of Applied Physics* **109**, 07D504 (2011).
- ¹³ J. H. Franken, M. Hoeijmakers, R. Lavrijsen, and H. J. M. Swagten, *Journal of Physics: Condensed Matter* **24**, 024216 (2012).
- ¹⁴ J. Ferré, T. Devolder, H. Bernas, J. P. Jamet, V. Repain, M. Bauer, N. Vernier, and C. Chappert, *Journal of Physics D: Applied Physics* **36**, 3103 (2003).
- ¹⁵ T. Gerhardt, A. Drews, and G. Meier, *Journal of Physics: Condensed Matter* **24**, 024208 (2012).
- ¹⁶ R. Lavrijsen, J. H. Franken, J. T. Kohlhepp, H. J. M. Swagten, and B. Koopmans, *Applied Physics Letters* **96**, 222520 (2010).
- ¹⁷ A. Kirilyuk, J. Ferré, V. Grolier, J. Jamet, and D. Renard, *Journal of Magnetism and Magnetic Materials* **171**, 45 (1997).
- ¹⁸ J. H. Franken, H. J. M. Swagten, and B. Koopmans, *Nature Nanotechnology* **7**, 499 (2012).
- ¹⁹ N.-H. Kim, D.-S. Han, J. Jung, J. Cho, J.-S. Kim, H. J. M. Swagten, and C.-Y. You, *Applied Physics Letters* **107**, 142408 (2015).
- ²⁰ T. Vemulkar, R. Mansell, A. Fernández-Pacheco, and R. P. Cowburn, *Advanced Functional Materials* **26**, 4704 (2016).
- ²¹ The code is available at www.srim.org.
- ²² S. Bandiera, R. C. Sousa, B. Rodmacq, and B. Diény, *IEEE Magnetics Letters* **2**, 3000504 (2011).